Originalarbeit

Berg Huettenmaenn Monatsh (2025) Vol. 170 (3): 132–139
https://doi.org/10.1007/s00501-025-01559-8

BHM Berg- und Hüttenmännische Monatshefte

Process Development and Risk Assessment for Processing Magnesium Alloys Using LPBF Technology

Franz Haas[1], Raphael Tiefnig[1], Marcel Braun[2], Michael Taschauer[3], and Stephan Steinacker[4]

[1]Graz University of Technology, Graz, Austria
[2]Paderborn University, Paderborn, Germany
[3]AdditiveXperts GmbH, Gumpoldskirchen, Austria
[4]Almamet GmbH, Ainring, Germany

Received December 19, 2024; accepted February 3, 2025; published online February 11, 2025

Abstract: Lightweight design is very closely associated with additive manufacturing. Besides the design possibilities offered by this technology, the material used also plays a key role. Especially in the LPBF process, the production of the powder and the processing of the material is a major challenge. This applies in particular to magnesium alloys as a lightweight material. Due to its low density and good strength and rigidity properties, this material is ideal for lightweight engineering applications. The basis of this contribution is a risk assessment (including a detailed FMEA and measures to minimize risks) for the processing and handling of magnesium powder in the LPBF process. As part of the practical tests, several test specimens with existing parameters for AZ91D were printed, and their properties (relative density, microstructure and bonding behaviour) were analysed. By adjusting the alloy composition (improved evaporation characteristics) and optimizing the process (e.g. optimum inert gas flow, platform temperature) and the process parameters, it is possible to process magnesium more economically in the LPBF process.

Keywords: Magnesium alloys, Additive manufacturing, Laser Powder Bed Fusion, Risk assessment, Process optimsation, Parameter development, Lightweight

Prozessentwicklung und Risikobewertung für die Verarbeitung von Magnesiumlegierungen mittels LPBF-Technologie

Zusammenfassung: Der Leichtbau ist sehr eng mit der additiven Fertigung verbunden. Neben den Gestaltungsmöglichkeiten, die diese Technologie bietet, spielt auch das verwendete Material eine wichtige Rolle. Gerade beim LPBF-Verfahren ist die Herstellung des Pulvers und die Verarbeitung des Werkstoffs eine große Herausforderung. Dies gilt insbesondere für Magnesiumlegierungen als Leichtbauwerkstoff. Aufgrund der geringen Dichte und der guten Festigkeits- und Steifigkeitseigenschaften eignet sich dieser Werkstoff ideal für Leichtbauanwendungen. Grundlage dieses Beitrags ist eine Risikobewertung (einschließlich einer detaillierten FMEA und Maßnahmen zur Risikominimierung) für die Verarbeitung und Handhabung von Magnesiumpulver im LPBF-Prozess. Im Rahmen der praktischen Versuche wurden mehrere Probekörper mit bestehenden Parametern für AZ91D gedruckt und deren Eigenschaften (relative Dichte, Gefüge und Anbindungsverhalten) analysiert. Durch Anpassung der Legierungszusammensetzung (verbesserte Verdampfungseigenschaften) und Optimierung des Prozesses (z. B. optimaler Inertgasstrom, Plattformtemperatur) und der Prozessparameter ist es möglich, Magnesium im LPBF-Prozess wirtschaftlicher zu verarbeiten.

Schlüsselwörter: Magnesiumlegierungen, Additive Fertigung, Laser Powder Bed Fusion, Risikobewertung, Prozessoptimierung, Parameterentwicklung, Leichtbau

1. Introduction

Magnesium, with a density of 1.75 kg/dm^3, is currently the lightest construction metal that can be used in industrial applications. Due to its good strength properties, this metal is particularly suitable for lightweight applications in modern mechanical engineering. In addition, the biocompatibility of magnesium also makes it suitable for use in medical engineering. Due to the low corrosion resistance of pure magnesium, the metal is mainly used in the form of magnesium alloys. Currently, most existing magnesium alloys

R. Tiefnig (✉)
Graz University of Technology,
Graz, Austria
raphael.tiefnig@tugraz.at

(>90%) are processed by die-casting and include more than 4% aluminium. Aluminium-free magnesium alloys are processed in sand or gravity die-casting, for example [1]. This allows the production of a wide variety of housing parts and engine blocks in large quantities. With the rise of metal additive manufacturing as a process for the production of complex components for industrial applications, the use of magnesium alloys in additive manufacturing (AM) offers additional weight reduction. Additive manufacturing of magnesium alloys is demonstrated in the literature using processes such as Powder Bed Fusion (PBF), Wire Arc Additive Manufacturing (WAAM), Paste Extrusion Deposition (PED), and Jetting Technologies (JT) [2]. This contribution investigates the processing of the magnesium alloy AZ91D in the LPBF process and takes a closer look at the challenges that arise.

As part of the Mg4AM research project, which runs until 2025, the Institute of Production Engineering (Graz University of Technology) and the Department of Materials Science (Paderborn University) are working together with three industrial partners (Almamet GmbH, AdditiveXperts GmbH and Schiebel Elektronische Geräte GmbH) to develop alloys for processing magnesium in the LPBF process.

In the LPBF process, the starting material is a fine metal powder (particle sizes 10–100 µm). The surface area to volume ratio results in a significantly higher hazard potential than with materials in wire form, for example. The following parameters are used to characterise the ignitability of materials: maximum explosion pressure (P_{max}), maximum rate of pressure rise $(dp/dt)_{max}$, minimum explosive concentration (MEC), minimum ignition temperature (MIT), minimum ignition energy (MIE), and limiting oxygen concentration (LOC) [3]. The particle size is decisive, as MEC and MIE increase significantly with an increasing particle size, which reduces the reactivity and explosion risk of the powder (Fig. 1; [4]). Another important factor, although difficult to measure, is the oxide layer of the powder particles. As the thickness of the layer increases, the reactivity of the powder decreases, but an oxide layer that is too thick makes it more difficult to melt the powder in the LPBF process.

Apart from the particle size, temperature, moisture content, pressure, and contaminants also have a significant influence on the ignitability of magnesium powders [5]. According to these assessment criteria, magnesium and magnesium alloys with a high magnesium content (>90%) are classified as materials with a moderate to high explosion hazard, again depending on the particle size and chemical composition [6, 7]. Due to the high hazard potential of magnesium powder in the LPBF process, safety measures must be observed along the entire process chain.

In addition to the safety aspect, the process parameters are a decisive factor. On the one hand, the strong smoke emission significantly complicates the LPBF process. The use of a more powerful gas flow pump is described in the literature as a possible solution [8, 9]. On the other hand, the high cooling rates in the LPBF process, together with the susceptibility of magnesium alloys to hot cracking, represent a further challenge [10, 11].

2. Materials and Methods

2.1 Risk Assessment

In order to detect and assess potential hazards when processing magnesium alloys in the LPBF process, all process steps were examined as part of a detailed FMEA and possible errors were derived. The project team evaluated these errors with a risk priority number. Values ranging from 1–10 were assigned to evaluate each defect using the three factors Occurrence (O), Severity (S), and Detection (D). The multiplication of these three factors provides the risk priority number (RPN) of a failure. The limit value was set at an RPN of 120. If the value was higher than this limit, appropriate measures were defined to reduce the RPN (<120) of a fault.

2.2 LPBF Process

The print jobs were carried out on an SLM 280 HL from Nikon SLM Solutions AG. The machine is equipped with a 400 W Ytterbium continuous wave fibre laser with a spot size diameter of 80 µm and has a wavelength of 1070 nm. The inert gas used for the process is argon. In order to minimise the powder volume in the process (measure from FMEA), an additional build envelope reduction unit was

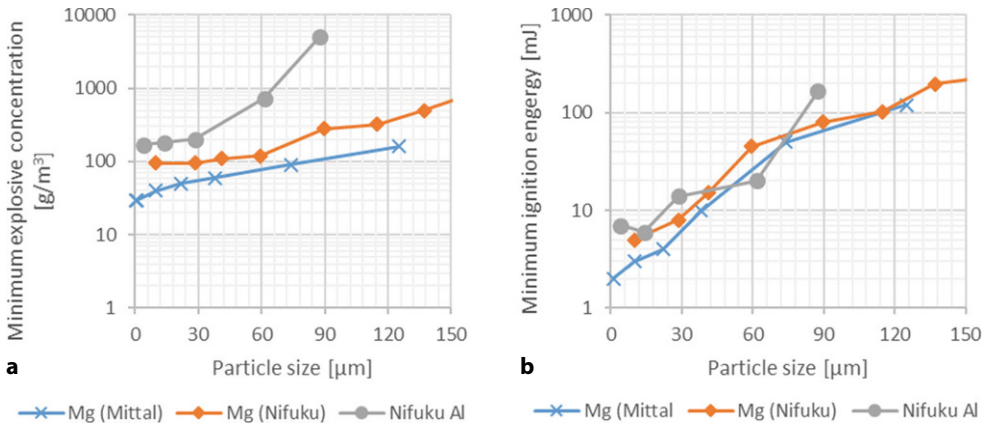

Fig. 1: Influence of particle size on the MEC (**a**) and MIE (**b**) for aluminium and magnesium [14]

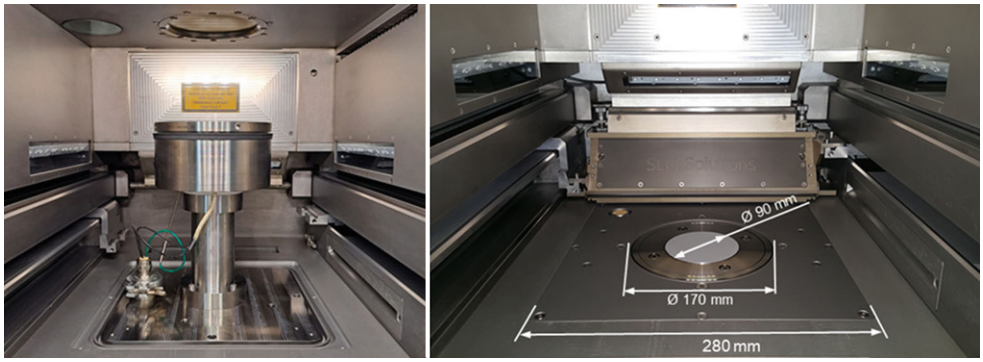

Fig. 2: Modification of the build volume by installing the build space reduction

used in the machine's build chamber (Fig. 2). This reduces the build volume filled with loose powder from 280 mm × 280 mm × 360 mm to a diameter of 170 mm × 110 mm. However, the available printing area is now only 90 mm in diameter due to the significantly smaller build platform.

A cylindrical plate made of AZ91 serves as the build platform. The coating width of the coater is narrowed by the installation of inserts. In addition, a barrier plate blocks one side of the coating chambers. Powder is only applied during the reverse movement. In addition to the machine's existing oxygen sensors, an external measuring device (Linde Gas GmbH) monitored the oxygen and moisture content in the build chamber. This allows the oxygen and humidity values to be measured and recorded in the ppm range. The PSM 100 sieving station (Nikon SLM Solutions GmbH) sieves the used powder during the post-processing. A vacuum cleaner with a water bath separator (AMC 300 from Nikon SLM Solutions GmbH) is used to clean the machines and ensure a safe disposal of the powder residues. For an additional passivation of the magnesium dust, a cooling lubricant is used in a concentration of 6–8% in the water bath of the vacuum cleaner and in the container for storing the magnesium waste.

2.3 Gas Flow Optimisation

CFD simulations form the basis for optimizing the inert gas flow in the build chamber. In addition to the standard configuration, various nozzle variants were tested in advance by using the software SimScale. A CAD model of the SLM machine's build chamber was also created for the simulations with the software Onshape. The inlet nozzles were printed using the FFF process on an Ultimaker S5 machine. The materials used for the nozzles were PLA and Tough PLA.

2.4 Alloy Development

The literature research showed that only a few standard alloys (AZ91, ZK60, and WE43C) have been printed so far [12]. The alloy ZK60 in particular is highly vulnerable to hot cracking and therefore has poor processability in the L-PBF process. For the alloy development, 14 alloying elements were analysed more closely and evaluated with regard to the known influences on magnesium as well as toxicity and price. Of these, eight alloying elements (Al, Ca, Mn, Si, Sn, Sr, Zn, Zr) were selected and characterised with regard to their influence on the evaporation behaviour. Based on the known phase formation and the expected properties, the following alloy systems (Fig. 3) were initially selected:

- Mg-Al-Mn
- Mg-Al-Ca-Mn
- Mg-Al-Si
- Mg-Al-Sr
- Mg-Sn
- Mg-Sn-Al

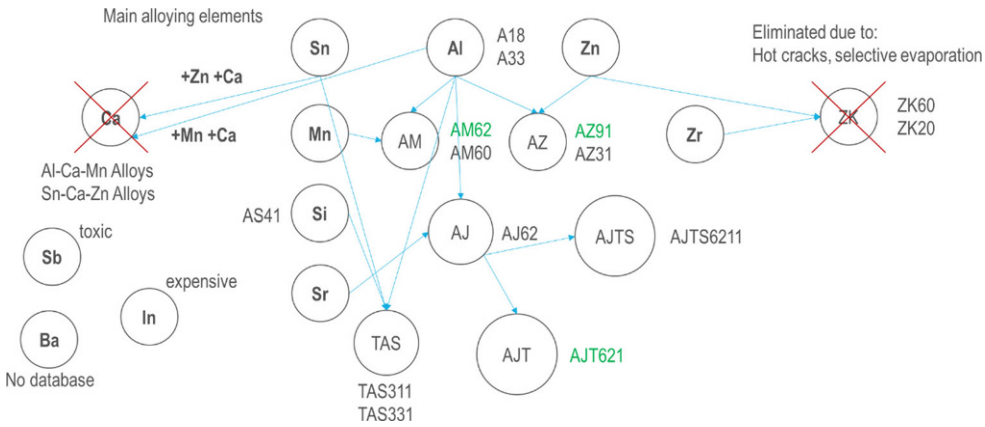

Fig. 3: Overview of the alloy development for the Mg4AM project

TABLE 1
Chemical composition of the AZ91D alloy

Element	Mg	Al	Cu	Zn	Be	Mn	Ni	Si
wt.%	90.40	8.93	0.0008	0.4294	0.001	0.19	0.003	0.029

The print jobs with AZ91D powder provided important insights for the alloy development. The evaporation tests showed that higher aluminium contents are recommended, but AZ91D with an aluminium content of just under 9% showed strong evaporation behaviour (smoke emission) during the LPBF process. The alloy composition alone is not sufficient to enable the processing of magnesium in this AM process. The areas of powder production (oxide layer formation/passivation) and process control are also significantly involved. Influencing the oxide layer or passivation of the powder particles is essential to enable subsequent processing in the LPBF machine. Song et al. show the formation of oxide layers on magnesium by the alloy partner lithium [13]. The influence of the alloy partners on the oxide layer, in particular on their melting points, is important for the LPBF process. Due to the high risk posed by Mg-Li alloys, these are not being pursued further in the project. However, further research activities in the project might be focussing on a possible Mg-Ba alloy as another candidate for the LPBF process, which could have a similar effect on the oxide layer of the magnesium alloy.

2.4.1 AZ91D Powder

The magnesium powder AZ91D was provided by Almamet GmbH and has the following chemical composition (see Table 1).

The powder particle distribution of this powder has the following results: D_{10} 24.67 µm, D_{50} 40.82 µm, and D_{90} 61.32 µm.

2.5 LPBF Process Parameter

A literature search was carried out to narrow down the parameter window [14–18]. When creating the individual parameter sets, the laser power (50–300 W), the layer thickness (30–120 µm), the laser speed (400–1050 mm/s), the hatch distance (0.045–0.09 mm), and the focus shift (0 to –8 mm) were varied. A bidirectional scanning strategy was used for the exposure, whereby the scanning direction was rotated by 67° after each layer. The parameters were assessed by visual inspection of the print results and by measuring the relative density of the test specimens.

Table 2 provides an overview of the process parameters from the literature, forming the basis for further parameter development.

2.5.1 AZ91 Bulk Samples

For theparameter development for AZ91D, several print jobs with cubic test specimens were performed. The test specimens were printed with a cross-sectional area of 15 × 15 mm and a height of 16 mm. Each print job included between 7 and 9 cubes with different parameters.

3. Results and Discussion

3.1 FMEA

Due to the high hazard potential of magnesium powder in the LPBF process, safety measures must be observed along the entire process chain. As part of an FMEA, possible faults were identified and their risk potential reduced through the use of suitable measures. Almost 40 possible faults had been identified and assessed, using a risk priority number (RPN).

However, the greatest risk is posed by the ignitability of the powder. For this reason, detailed work instructions (checklists) have been drawn up as a general measure for carrying out Mg printing jobs. Another action is the use of ESD equipment and tools for working on the machine. An external sensor system is used to monitor the oxygen and moisture level in the build chamber during the printing process in order to rule out possible malfunctions (redundancy). The powder handling during the post processing happens in an inert gas atmosphere with the build chamber door closed.

Thanks to these and other measures, the RPNs of all detected failures were reduced below the specified limit in order to create the desired framework for working with magnesium alloys.

TABLE 2
AZ91D process parameter from the literature

Name	Layer thickness [µm]	Laser power [W]	Laser speed [mm/s]	Hatch distance [mm]	Focus [mm]	Volumetric energy density [J/mm^3]	Build-up rate [cm^3/h]
Aconity 3D AZ91D [16]	30	200	700	0.06	0	158.73	4.5
Schmid [19]	30	162	700	0.063	0	122.45	4.8
Jau19-P1 [20]	30	100	800	0.04	0	104.17	3.5

3.2 Smoke Emission

The first printing tests with AZ91D have confirmed the findings from the literature. The processing of AZ91D in the LPBF process leads to a very strong smoke emission and requires additional measures to make efficient printing possible. The resulting process smoke influences the laser beam during the scanning and, over time, increasingly settles on the laser entrance window and clouds it.

3.2.1 Skywriting

The first parameter tests required skywriting operations to create additional exposure pauses. For this purpose, dummy cubes were placed on the platform, which were exposed with a laser power of 0 W and a scanning speed of 950 mm/s. During these pauses, the process smoke in the build chamber could be evacuated to ensure appropriate process conditions for the next exposure step. These pauses (approx. 70% of the duration of the previous exposure step) were necessary due to the high smoke emission during processing of the laser, but lead to a significantly longer printing time.

3.2.2 Gas Nozzles

Due to the long printing time caused by the additional skywriting operations, inlet nozzles were developed to improve smoke evacuation. The existing flow situation in the build chamber was modelled using CFD simulation. The gas flow was optimised for the modified powder bed in order to convey the process fumes as efficiently as possible to the outlet opening of the build chamber. The best results were achieved with two nozzles on the inlet side (Fig. 4). Nozzle 1 guides the gas flow over the powder bed and forces the fumes towards the outlet opening. Nozzle 2 prevents the fine smoke particles from settling on the laser entrance window and blows the rising smoke down towards the outlet. By using the inlet nozzles, the pump capacity (from 60–40%) and gas velocity (from 6–3.2 m/s) had to be adjusted compared to the standard configuration in order to prevent the powder from being blown away from the powder bed. These gas speed settings were determined by practical tests in the build chamber.

By using the gas inlet nozzles, the majority of the process fumes are immediately removed from the build chamber, which means that the use of dummy cubes or skywriting operations can be skipped for the build job preparation. The exposure time per layer in the production of nine of the test specimens described is reduced by 40%, which leads to a significant reduction in the overall build time.

3.3 AZ91D Test Specimen

The parameter sets AX22–AX30 (Fig. 5) formed the basis for further investigations with regard to the microstructure of the cubes. The volumetric energy density (E_v) used, can be calculated using Eq. 1 and includes laser power (LP), laser speed (LS), layer thickness (LT) and hatch distance (HD). This generates a process window between 78.9 and 142.5 J/mm^3.

$$E_v = \frac{LP}{LS*LT*HD} \tag{1}$$

The theoretical build-up rate (BR_{th}) can be calculated using the following equation:

$$BR_{th} = LT*LS*HD \tag{2}$$

It ranges from 6.3–9.1 cm^3/h for the parameters AX22–AX 30.

After several print jobs, the AZ91D powder was analysed again, and the following powder distribution values were found: D_{10} 25.355 µm, D_{50} 43.792 µm, and D_{90} 74.109 µm. A slight increase in grain size of the powder due to the printing processes can therefore be recognised.

3.3.1 Bonding Behaviour

Initial printing tests with an aluminium substrate plate showed a poor bonding of the test specimens. With an in-

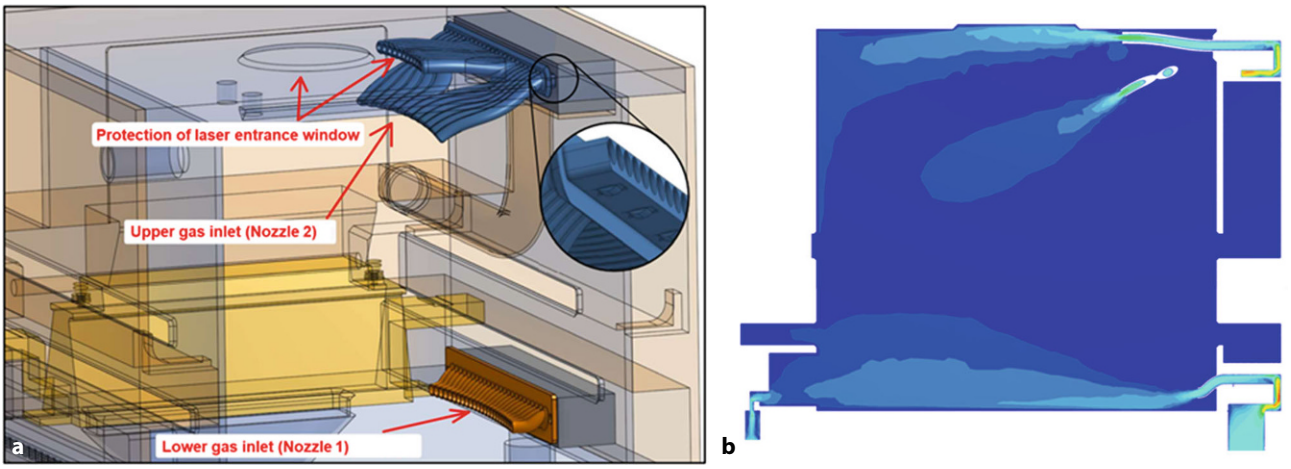

Fig. 4: Build chamber with additional nozzles (**a**) and the resulting inert gas flow (**b**)

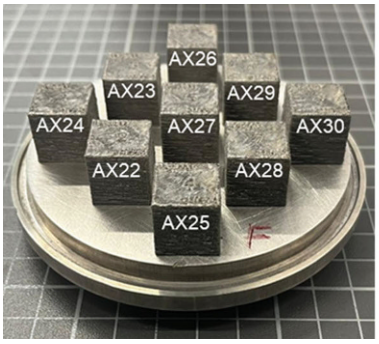

a

Nr.	Name	Layer thickness [µm]	Volumetric energy density [J/mm³]	Build-up rate [cm³/h]
1	AX22	60	114.0	6.3
2	AX23	60	93.2	7.7
3	AX24	60	78.9	9.1
4	AX25	60	128.2	6.3
5	AX26	60	104.9	7.7
6	AX27	60	88.8	9.1
7	AX28	60	142.5	6.3
8	AX29	60	116.6	7.7
9	AX30	60	98.6	9.1

b

Fig. 5: Array of the test specimens (AZ91D) on the substrate plate (**a**) and overview of the process parameters (**b**)

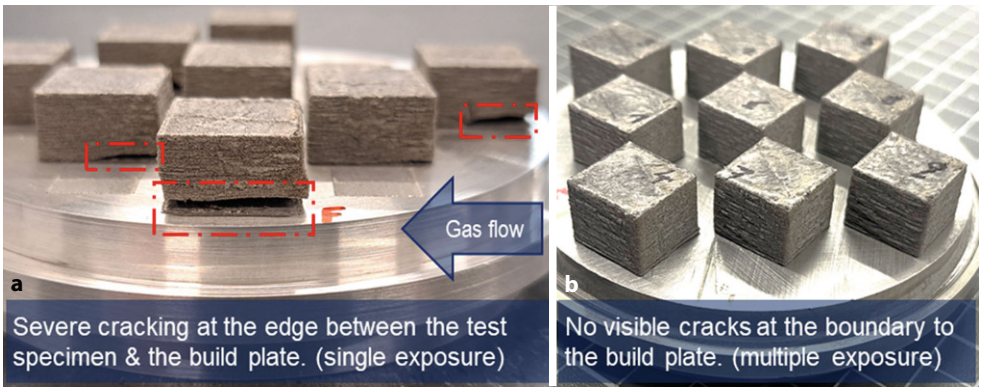

Fig. 6: Bonding behaviour influenced by the initial exposure of the laser

creasing build height, the adhesion was no longer sufficient and the parts became detached. This bonding problem occurred both with and without platform heating (100 °C). Subsequently, substrate plates made of AZ91 were used for the print jobs. With a platform temperature of 150 °C and a double initial exposure (triple exposure) of the first layer, a very good bond to the substrate plate was achieved. No cube detached during the entire print job. The multiple exposure of the first powder layer results in a good bonding to the substrate plate, which is a clear improvement on the tests with single exposure, where noticeable cracking (Fig. 6a) can be seen in the first layers.

3.3.2 Relative Density

Microscopic analyses (Fig. 7) of the printed samples show porosities in the range of 0.26–0.99%. The best result is achieved by the AX25 sample with a relative density of 99.74%. This sample also shows hardly any inclusions. With a volumetric energy density of 128.2 J/mm, this also confirms the results of the literature, which show that when processing magnesium alloys in the LPBF process, higher energy densities tend to lead to a higher relative density of the component.

Another conclusion from the print jobs with AZ91D is the influence of the process fumes and the oxygen content in the build chamber on the porosity of the test specimens. In the microstructure (Fig. 8) of the specimens with a higher smoke concentration in the build chamber (print job with dummy cubes without gas nozzle) with comparable printing parameters, there are more pores than the specimens printed with the optimized gas flow. The sample AX17 has a porosity of 2.91%, while AX22 shows a value of 0.93%. This emphasizes the negative influence of smoke on the printing process and the print result.

3.3.3 Electron Microscopy

The electron microscopy of two printed AZ91D cubes shows the influence of oxides on pore forming in the printing process. In Fig. 9, more oxides (green in the mapping) can be seen at the edges of the pores. If the energy density is too low ($E_v < 100$ J/mm^3) and the oxide layer on the powder is too thick, this leads to higher porosity in the samples and incomplete melting of the powder particles. First microstructural analyses of the AZ91D samples also show fine-grained microstructure typical of the LPBF process.

4. Conclusion

The research activities carried out in the field of additive manufacturing of magnesium alloys using the LPBF process ranged from the identification of safety measures for the processing and handling of Mg powder to process optimisation and parameter development for two AZ91D. The tests carried out have revealed the following findings:

- Due to the high reactivity of magnesium powder, handling in pre- and post-processing is only advised if appropriate safety measures are observed. The exclusion of atmospheric oxygen, sufficient passivation of

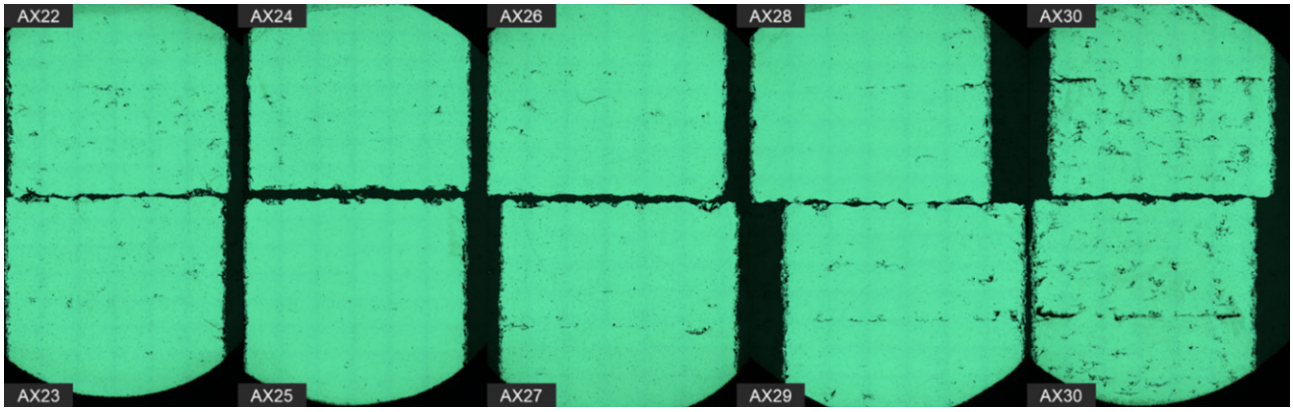

Fig. 7: Micrographs of the AZ91D test specimens AX22–AX30

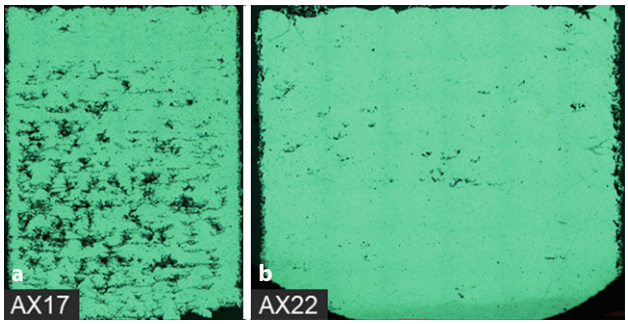

Fig. 8: Influence of process smoke on the microstructure of the samples, without gas nozzle (**a**) and optimised gas flow (**b**)

the powder and powder waste are crucial. Thanks to the measures resulting from the FMEA, the risk of possible failures could be reduced in order to enable safe processing.

- The intense smoke emission during the exposure process significantly limits the processability using the standard configuration of the SLM 280 HL. An optimised inert gas flow is required to keep the build chamber and the laser entry windows free of fumes. The use of the gas nozzles has significantly improved smoke removal, leading to shorter printing times (reduction by 30–40%) on the one hand and better results in terms of porosity (increase from 2.91–0.93%) on the other.
- The exposure process in the first layer is crucial for the bonding behaviour of the components to the substrate plate. Multiple exposures create a sufficient adhesion for a stable printing process.
- Relative densities of up to 99.74% were achieved with AZ91D. In addition to the process parameters (E_v), the oxygen content and the process smoke in the build chamber also had a significant influence on the porosity of the samples. The measured oxygen content during the printing (<700 ppm) was below the limit value of 0.1% specified by the machine control.
- The magnesium oxides cause the expected difficulties in the production of non-porous components. However, the fine-grained structure created by the printing process promises good mechanical properties.

The next stage of the project involves similar tests with two other magnesium alloys in order to use the best results for the production of the first demonstrator components through further parameter optimisation. At the same time,

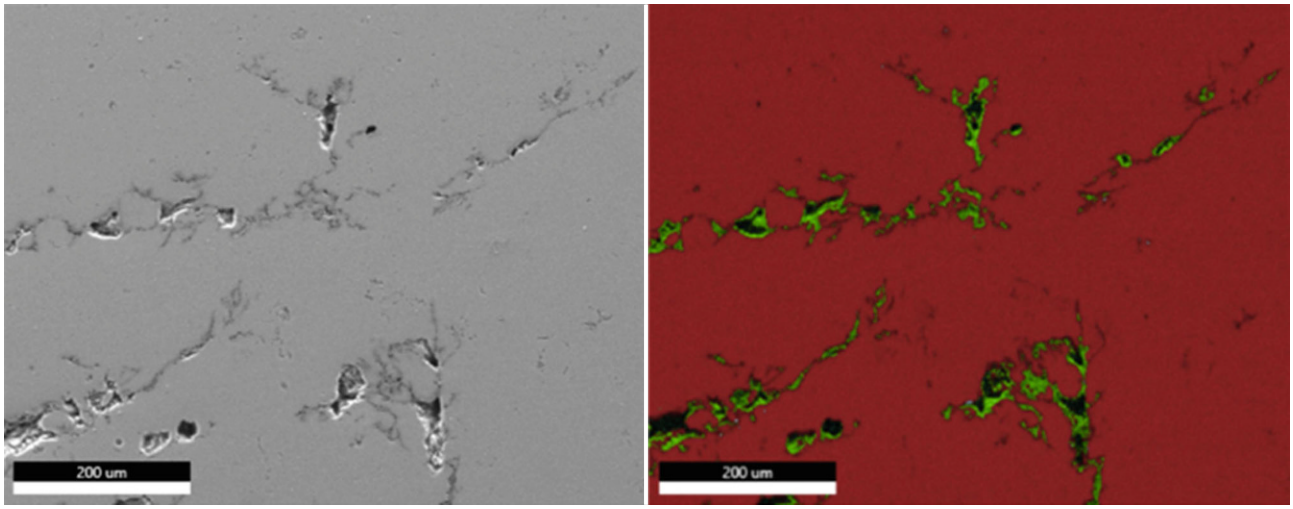

Fig. 9: Influence of oxides on pore formation in a printed AZ91D sample

further analyses of the microstructure of the already printed samples and the investigation of their chemical compositions are being carried out.

Funding. The research activities were carried out as part of the Mg4AM project (Project number: FO999895334). The project is part of an IraSME call, a network of national and regional funding programmes to support transnational research and development cooperation between small and medium-sized enterprises and research institutions. The authors would like to thank the Austrian Research Promotion Agency (FFG) and the German Central Innovation Programme for SMEs (ZIM) for their financial support.

Funding. Open access funding provided by Graz University of Technology.

References

1. Dieringa, H., Bohlen, J.: Magnesiumlegierungen im Leichtbau (2017). https://www.konstruktionspraxis.vogel.de/magnesiumlegierungen-im-leichtbau-a-552075/, Accessed 29 July 2024
2. Sealy, M.P., Karunakaran, R., Ortgies, S., Tamayol, A., Bobaru, F.: Additive manufacturing of magnesium alloys. Bioact. Mater. , 44–54 (2020)
3. Gang, L., Chunmiao, Y., Peihong, Z., Baozhi, C.: Experiment-based fire and explosion risk analysis for powdered magnesium production methods. J Loss Prev Process Ind , 461–465 (2008)
4. Nifuku, M., Koyanaka, S., Ohya, H., Barre, C., Hatori, M., Fujiwara, S., Horiguchi, S., Sochet, I.: Ignitability characteristics of aluminium and magnesium dusts that are generated during the shredding of post-consumer wastes. J Loss Prev Process Ind , 322–329 (2007)
5. Mittal, M.: Explosion characteristics of micron- and nano-size magnesium powders. J Loss Prev Process Ind , 55–64 (2013)
6. Neikov, O.: Safety engineering in the production of powders. In: Handbook of non-ferrous metal powders, pp. 551–595. (2009)
7. Guide to Legislation and "Health and Safety" in the European PM, EPMA, (1997).
8. Nopová, K., Jaroš, J., Červinek, O., Pantělejev, L., Gneiger, S., Senck, S., Koutny, D.: Processing of AZ91D magnesium alloy by laser powder bed fusion. Appl. Sci. , (2023)
9. De Smit, M., Paesano, A., Montero-Sistiaga, M., Velterop, L.: Development of magnesium laser powder bed fusion to manufacture light-weight components for vertical lift applications. Forum 77—The Future of Vertical Flight. (2021)
10. Zhong, H., Lin, Z., Han, Q., Song, J., Chen, M., Chen, X., Li, L., Zhai, Q.: Hot tearing behavior of AZ91D magnesium alloy. J. Magnes. Alloy. , (2023)
11. Song, J., Pan, F., Jiang, B., Atrens, A., Zhang, M., Lu, Y.: A review on hot tearing of magnesium alloys. J. Magnes. Alloy. , 151–172 (2016)
12. Zeng, Z., Salehi, M., Kopp, A., Xu, S., Esmaily, M., Birbilis, N.: Recent progress and perspectives in additive manufacturing of magnesium alloys. J. Magnes. Alloy. , 1511–1541 (2022)
13. Song, Y., Shan, D., Chen, R., Han, E.-H.: Investigation of surface oxide film on magnesium lithium alloy. J Alloys Compd , 585–590 (2009)
14. Schmid, D.: Untersuchungen zum Laserstrahlschmelzen von Magnesiumlegierungen (2020)
15. Wei, K., Gao, M., Wang, Z., Zeng, X.: Effect of energy input on formability, microstructure and mechanical properties of selective laser melted AZ91D magnesium alloy. Mater. Sci. Eng. , 212–222 (2014)
16. Aconity 3D, Data sheet AZ91D, 2020.
17. Li, X., Fang, X., Wang, S., Wang, S., Zha, M., Huang, K.: Selective laser melted AZ91D magnesium alloy with superior balance of strength and ductility. J. Mangesium Alloy. , (2022)
18. Ahmadi, M., Bozorgnia Tabary, S., Rahmatabadi, D., Ebrahimi, M.S., Abrinia, K., Hashemi, R.: Review of selective laser melting of magnesium alloys: advantages, microstructure and mechanical characterizations, defects, challenges, and applications. J. Mater. Res. Technol. , 1537–1562 (2022)
19. Schmid, D., Renza, J., Zaeh, M.F., Glasschroeder, J.: Process influences on laser-beam melting of the magnesium Alloy AZ91. Phys Procedia **83**, 927–936 (2016)
20. Jauer, L.: Laser Powder Bed Fusion von Magnesiumlegierungen (2018)